IR HORIZON PHENOMENOLOGY: REPORT ON IRAMMP FIELD TEST

January, 1991

E.H. Takken, R.G. Priest, E.P. Shettle and J.C. Kershenstein
Naval Research Laboratory
Washington, DC 20375

ABSTRACT

An IRAMMP field measurement exercise was conducted during July 1990 in the Florida Keys. The purpose of the exercise was to investigate horizon radiance phenomenology and associated clutter structure. In the exercise both the IRAMMP sensor and a PtSi imager were used. The sensors were located 31 m above the surface of the water in a ocean side apartment building. The IRAMMP sensor is a dual band 120 element radiometric scanner with an IFOV of 250 microradians. The PtSi sensor was a commercial staring instrument with a 85 microradian IFOV. High quality digital data were obtained on a number of days and nights over a three week time span. In most of the data sequences a bright IR point source on a small boat was observed as it transited over the horizon. The precise range to the point source was recorded at all times. An excellent set of meteorological "ground truth" data was collected in conjunction with a parallel NRL/NOSC field exercise called KEY90.

This paper is a partial report on results obtained from the analysis of data from the Florida field measurements. Emphasis in this paper will be on three aspects of the low horizon phenomenology. These are: 1) the form of the radiance profile singularity in the vicinity of the horizon line, 2) the appearance of a point source as it traverses the horizon, and 3) the solar glitter pattern seen on the water under a favorable illumination geometry.

1.0 INTRODUCTION

One of the goals of the IRAMMP program is collection of background clutter data sets that can be used as test beds for various clutter models. A background of specific military significance is the air-sea horizon. Of particular importance is the angular region within a few milliradians of the horizon line. Three issues of background phenomenology have been identified as having primary importance for this background. These are: 1) The form of the radiance angular profile in the vicinity of the horizon line, 2) The appearance of point sources as they cross over the horizon, 3) The statistical structure of the clutter field caused by solar glitter on the surface of the water near the horizon.

In order to acquire high quality horizon data, an IRAMMP field test was

conducted in the Florida Keys during July, 1990. The Florida Keys site was selected because the ocean to the south of the island chain is minimally affected by land masses and is thus is representative of the open ocean. The IRAMMP scanning sensor was located on a ocean front balcony 31 m above sea level. With this elevation, the horizon is approximately 20 km from the sensor. The water at 20 km is well past the reef line and is thus representative of deep water conditions. The July time frame for the test was selected so that it would coincide and be collocated with a multi-laboratory aerosol measurement field exercise called Key 90[1] . This arrangement had the advantage that a rather complete set of "ground truth" meteorological data was available. The data include those from a weather station, an instrumented air plane and two 10 meter size small boats. The meteorological data collected with this instrumentation provides crucial input to the clutter models discussed later in this report.

A visible telescope/camera was located along with the IRAMMP sensor in the ocean front apartment. The telescope had an IFOV of 20 microradians and was useful for gauging image wander effects due to turbulence. The other principal apparatus used in the field test was an IR source mounted on a 30 ft boat. The source was a propane fired 6" by 9" ceramic heater element operated at a temperature of near 1000 C. The source provided a signature of approximately 100 watt/sr in the 3.8 -4.9 micrometer band. The boat was equipped with a loran unit capable of giving range with respect to the shore station accurate to about 0.1 km. These ranges were communicated to the shore station via radio.

The IRAMMP sensor simultaneously measures the radiances in two IR channels (LW and MW). The recorded images cover a 1.7 by 5.6 degree field of view with a 0.25 milliradian pixel resolution. IRAMMP data was recorded with the sensor scanning vertically. This orientation places the scan direction, which is oversampled by a 3 to 1 ratio[2], along the direction of most variation in the background. In cases where the boat with the IR source was deployed, a boresighted rifle scope was used to acquire the boat at close range. The boat was driven on a radially outward course and kept in the field of view of the IRAMMP sensor by changing the azimuthal pointing direction of the sensor as required. As the boat neared the horizon, an oscilloscope display derived from the sensor was used as a cue for pointing the sensor. The signal to noise ratio of the source rarely dropped below 3 to 1 until the source transited over the horizon.

Data were recorded with five main objectives. First, to acquire angular radiance profiles of the horizon under a variety of conditions. Second to observe the dynamics of the appearance of a point source as it traversed across the horizon. Third, to study solar glitter clutter structure. Fourth,

to determine the maximum range at which a point source could be observed as a function of meteorological conditions. Fifth, to obtain cloud clutter data on a opportunistic basis. This paper is a preliminary report on results obtained on the first three of these objectives.

All of the IRAMMP data discussed in this paper are available for general distribution. The distribution media is 9 track tape encoded with the NATO format[3].

2.0 ANGULAR RADIANCE PROFILES OF THE HORIZON

When an IR imaging sensor is pointed at the sea horizon, the resulting image is essentially a record of the radiance as a function of elevation angle. (There is no static structure in the azimuthal direction.) It has been recognized for some time that an analytic model of this radiance profile would be a valuable tool for extrapolating data and estimating the severity of clutter. Hughes[4] has developed an extensively modified version of the LOWTRAN code for this purpose. The modifications include a very fine layering of the first few meters of the atmosphere and the inclusion of a roughened sea surface. Unfortunately, the modified code is in preliminary form and is not generally available. We outline below a simpler approach, based on established code, that can account for most of the observed features of the radiance profiles seen in the Florida Keys exercise.

Our starting point is the division of the problem into two regions. For elevation angles above the horizon, the radiance is path radiance including scattered solar radiation. Modeling of this path radiance is a standard feature of LOWTRAN. For elevation angles below the horizon, there are three contributions: 1) path radiance for the section of the path between the sensor and the surface of the ocean, 2) thermal emission from the ocean, 3) reflected sky radiation. Modeling of the first term is again a standard LOWTRAN calculation. In the absence of whitecaps, modeling of the second term is straightforward if an effective reflectivity for the water surface can be established. Modeling of the third term poses additional difficulties. Is the reflection primarily diffuse or specular? If diffuse, should a wave slope statistics approach be used or should the surface be considered to be a perfect Lambertian diffuse reflector as standard LOWTRAN assumes[5]?

Under the conditions of the Florida Keys tests (negative air-sea temperature difference, gentle seas), the radiance profiles were generally continuous across the horizon with an apparent slope discontinuity at the horizon. This cusp-like feature is a clutter source which could potentially degrade the performance of a search algorithm. For this reason it is desirable to achieve an understanding of the cusp feature based on established

modeling tools such as LOWTRAN. Since it is the cusp feature itself which is the clutter source, a detailed understanding of the radiance profile is essential only for a few milliradians on either side of the horizon.

It appears to be plausible, and indeed the model calculations below support the idea, that the relatively large air temperature gradient in the last few meters above the sea surface is responsible for the cusp-like feature. The radiance is a maximum at the horizon because the horizon ray traverses the longest path in the air very near the water surface. This is the warmest layer of air for the condition of a negative air-sea temperature difference. Our modeling approach starts with the definition of a custom temperature profile for LOWTRAN. This profile has 3 layers in the first 10 meters above the surface. The detailed profile was derived from the model of Davidson et. al.[6], however substantially similar results would be obtained using the models of Walmsley[7] or Paulus[8]. It is given in Table 1. The critical input in this class of models is the air-sea temperature difference, which was taken to be -1 C. The ground truth data recorded during the test indicated that this value was present in a remarkable consistent manner during the duration of the test. This parametric choice is reflected in Table 1 in that the difference between the temperature at the surface and at 10 m is -1 C. Note that the surface temperature was taken as 29 C. This is close to the actual temperature observed during the during the test. The temperature profile was continued onto the LOWTRAN Mid-latitude summer profile in a smooth manner. The humidity profile was set at a constant value of 75% relative humidity. The actual humidity profile was higher, in the first few meters above the surface (approaching 100 % at the surface). LOWTRAN makes approximations in determining the aerosol attenuation when the relative humidity exhibits large variations within the boundary layer. Rather than risk possible artifacts from inclusion of such variations, we fix the humidity at 75%. Other LOWTRAN options selected were: multiple scattering, Navy Maritime aerosol model, windspeed (both current and 24 hr average) = 4 m/second, and ICSTL = 6 (2 day old aerosols). The visibility was defaulted to that of the Navy Maritime model (approximately 32 km for this choice of parameters).

Since we are interested in the radiance only in a very narrow angular region near the horizon, we can make several simplifying assumptions that are motivated in part by the observation that the radiance is continuous across the horizon. Since the water is warmer than the air, any thermal emission from the water at the horizon reaching the sensor would lead to a discontinuity in the observed radiance. Thus we assume that the water surface is a perfectly reflecting specular surface. This may appear to be a drastic assumption in light of the usual approach to this problem using, for example,

Table 1

Height (m)	Temperature (K)	Relative Humidity
0.0	302.0	75.0
1.0	301.241	75.0
5.0	301.124	75.0
10.0	301.0	75.0
20.0	300.87	75.0
30.0	300.75	75.0
40.0	300.64	75.0
50.0	300.54	75.0
60.0	300.44	75.0
80.0	300.24	75.0
100.0	300.04	75.0
200.0	299.04	75.0
300.0	298.04	75.0
500.0	296.10	75.0
1000.0	293.00	75.0
2000.0	287.00	75.0
3000.0	281.00	75.0
4000.0	275.00	75.0
5000.0	269.00	75.0
7000.0	256.00	75.0
10000.0	235.00	*
15000.0	*	*
20000.0	*	*
30000.0	*	*
50000.0	*	*
100000.0	*	*

* = LOWTRAN Mid-Latitude Summer Profile

Cox-Munk[9,10] wave slope statistics. However, any surface will become highly reflecting and specular for rays near enough to grazing incidence. In terms of the wave slope picture, all of the rays reflect off the very tops of the wave crests for incidence angles near grazing. The Fresnel equations guarantee a very high reflectivity for this case. With this assumption, thermal emission from the ocean makes little or no contribution to the observed radiance. The contribution from reflected sky radiance is equal to the radiance of the reflected ray (surface to space) multiplied by the band average transmission along the path from the sensor to the surface. Thus for rays below the horizon, the radiance equation is:

$$R_o(\theta) = R_p(\theta) + \tau(\theta) R_s(\theta') \qquad (1)$$

where $R_o(\theta)$ is the radiance seen by the sensor at the zenith angle θ, $R_p(\theta)$ is the radiance on the path from the sensor to the point at which the ray strikes the surface of the water, $\tau(\theta)$ is the average transmittance on that path and $R_s(\theta')$ is the sky radiance reaching the surface at the specular reflection angle θ'. The transmittance, τ, is a strong function of the angle principally

because the path from the sensor to the point where the ray strikes that water shortens as the zenith angle is lowered below the effective horizon. For angles above the horizon, the expression for the observed radiance is much simpler:

$$R_o(\theta) = R_{space}(\theta) \qquad\qquad (2)$$

where $R_{space}(\theta)$ is the radiance computed from Lowtran using the slant path to space option at the zenith angle θ. To insure that the observed radiance is continuous across the horizon, the value of R_s at the horizon, $R_s(\theta_h)$, must be such that Eq. (1), evaluated at θ_h yields the same value as Eq. (2) evaluated at θ_h. This condition can be checked within LOWTRAN. For the 8-12 band, consistency within 4% is obtained. For the midwave band, less consistent results (10 %) are obtained because of the fact that the transmittance is a band average while the sky radiance is not spectrally flat.

Implementation of the model of Eq. (1) and (2) is not difficult within the standard LOWTRAN 7 code[11]. To implement Eq. (2) the slant path mode is used with sensor height (31 m), ray angle and path to space specified. To implement Eq. (1) a slightly more complex procedure is followed. To calculate R_p, the slant path mode is used with sensor height, ray angle and target height, 0 m, specified. For this latter calculation, the water is "turned off" by specifying an albedo of zero and a surface temperature of 100 K. This is necessary because the standard LOWTRAN reflectance model is that of a Lambertian surface - inappropriate in this case. In addition to R_p, the LOWTRAN calculation provides τ and the incidence angle at which the ray strikes the surface. To calculate R_s, LOWTRAN is run to compute the sky radiance reaching the surface using the supplement of this incidence angle. It is necessary to make a small correction to this value as discussed in the previous paragraph. Finally Eq. (1) is used to calculate R_o.

The results of this calculation for the longwave case (7.8 - 11.9 micrometer) is shown as the dotted line in Fig. 1. The experimental LW radiance angular profiles for scenes 0195-009 (July 14, 1990), 0200-011, 0200-016, 0200-13 and 0200-022 (July 19, 1990), averaged over all 120 channels, are shown as solid traces in the same figure. It can been seen that the model calculation qualitatively reproduces the cusp structure seen in the experiment. The model slope discontinuity is sharper than the experimental values. The discrepancy may be due in part to the conservative value used for the relative humidity in the model calculation. Higher relative humidity leads to higher attenuation, which will reduce the radiance slope above the horizon (and perhaps also reduce the slope below the horizon). Increasing the aerosol attenuation would also tend to reduce the slope. The variation among

the maximum radiances seen in Fig. 1 is not significant. It reflects small temperature shifts on the order of 1 degree. While the average temperature varied on the order of a few degrees, the air-sea temperature was nearly always -1 C during the period of the field measurement exercise.

The situation is more complex for the midwave case because the scattered thermal radiation makes a much larger contribution to the observed radiance. However, there is also a significant thermal contribution. Therefore, the mechanism discussed above is able to produce a cusp-like feature in the radiance profile. Such a feature was seen in the majority of the scenes analyzed. Analysis of this data is in progress.

3.0 POINT SOURCE SCINTILLATION EFFECTS

The IR source used in this test was sufficiently small that it acts as an ideal point source when viewed at a range of 20 km. The IRAMMP sensor records the intensity of the source, integrated for 1/8800 sec, every 1/4 second. With appropriate subtraction of the background, the IRAMMP data can be represented as a time series of intensity points. All of the spectral power in point source scintillation is confined to frequencies far lower than 8800 Hz so the estimated variance of this time series is related to the variance in collected signal power calculated by standard turbulent scintillation theory. It is most convenient to work with variances normalized by the square of the means. The normalized variance of the time series is equal to the normalized variance of the collected signal power if the time series is long enough (10 seconds is adequate).

The theoretical formulation presented by Hufnagel in The Infrared Handbook[12] is convenient for obtaining the normalized variance in collected signal power, σ_S^2. The relevant formula is:

$$\sigma_S^2 = (\exp(4\sigma_\chi^2) - 1) f \qquad (3)$$

where σ_x^2 is the variance of a random variable related to electric field fluctuations. σ_x^2 is related to the index of refraction structure function, C_n^2, by

$$\sigma_\chi^2 = 0.124 C_n^2 k^{7/6} L^{11/6} \qquad (4)$$

where k is 2π divided by the wavelength and L is the path length. The factor f appearing in Eq. (3) represents the effect of aperture averaging. For a

very small sensor aperture, f=1. For the midwave region of the spectrum f is approximately 1/2 for the IRAMMP sensor aperture. (See figure 6-9 in ref. 12). Ref. 12 gives a value of 10^{-15} $m^{-2/3}$ for C_n^2 near the surface of the sea. More refined calculations based on the work of Davidson et al. for an air sea temperature difference of -1 C and wind speed of 4 m/sec predict a slightly lower value of 4 x 10^{-16} which is the value we use here. The path length L is taken as 20 km and the wavelength is taken as 4 micron. With these values Eq. (3) and (4) predict σ_s^2 = 0.18. This value is somewhat lower than the regime in which saturation effects invalidate Eq. (3). However it is sufficiently close to this region to warrant caution.

The time series of normalized intensities derived from IRAMMP sequence 0198-017 (July 17, 1990) is presented in Fig. 2. This data was collected using filter 6 (3.89 - 4.06 micrometer). The points are derived from a sequence of 42 consecutive forward scans (1/2 second apart). Each (unnormalized value) was obtained by summing the radiance values in a 9 x 3 pixel area centered on the target and then subtracting a similarly calculated background value. The background value was calculated by summing the radiance values in an equivalent 9 x 3 pixel area of the scan close to the area containing the source. The source was at a range of 21 km. Similar results were obtained by analysis of the data recorded by the PtSi sensor.

The normalized variance estimated from this time series is 0.270. It was possible to estimate the contribution to this variance coming from sensor noise by analysis of areas of the scan not containing a target. This contribution was found to be 0.018 which is much less than 0.27. The agreement between the model value for σ_s^2 , 0.18 and the experimental value, 0.270 - 0.018 = 0.252 is good enough to suggest that classical turbulence effects are indeed responsible for the observed source flicker. Only a small change from the modeled value of C_n^2 used is needed to gain complete agreement. Other possible reasons why the experimental value may be larger than the theoretical include: fluctuations in the source temperature due to puffs of wind, and changes in the viewing angle to the source due to changes in heading of the boat carrying the source. While it is not possible to quantify the size of these effects, they are thought to be small for the following reasons. The source was well shielded from the wind by a 2' x 3' x 3' box projecting out in front of it. The nominal viewing orientation of the source was normal to the line of sight. Thus fairly large changes in orientation are required to change the cosine of this angle by as much as 10 percent. Finally, the time sequence of Fig. 2 appears to be a white noise process. Changes in orientation, puffs of wind etc. would be expected to yield fluctuations with some evidence of correlated behavior.

4.0 SOLAR GLITTER CLUTTER

Solar glitter produces a highly cluttered background structure when the sensor views the horizon directly under the sun provided that the sun is low in the sky (lower than about 45 degrees zenith angle). The magnitude of this clutter source is highly dependent on elevation angle of the sun, azimuthal angle relative to solar azimuth, sensor pass band and degree of cloud cover. The most comprehensive modeling tool for this clutter source known to the authors is the SEABEAM code[13]. This code in its current form is limited to the visible region of the spectrum. However it should be possible to modify it to cover the midwave IR.

In the Florida Keys test, one systematic collection of solar clutter data was made. On July 19, 1990, day 200, a sequence of scans was recorded between 9:22 and 9:29 in the morning. The solar elevation angle was 36 degrees (54 degrees zenith angle). Scans were made at a series of azimuthal angles with respect to the solar azimuth. The radiance profiles are presented in Figs. 3 and 4. The IRAMMP scene numbers are: 0200-014 through 0200-021. The 3.89 - 4.06 micron band was used for these measurements. The reader will note that the solar glitter is highest for azimuths closest to the solar azimuth as expected. In some of the scans there is a spike at the horizon. This is due to the presence of broken cloud cover. The ocean surface close in (lower elevation angles) was in partial shade compared to the water surface 15 km and further out (at the horizon). The reader will note that in Fig. 4c and 4d, the radiance above the horizon is higher than the radiance below the horizon. There is a radiance discontinuity at the horizon. This is an atypical situation (based on analysis of other data from the test). There is evidence that it is due to a very low lying aerosol layer.

Analysis of these profiles is ongoing. One general observation can be made at this point. The presence of scattered clouds can have a major impact on the glitter structure.

5.0 STATUS AND SUMMARY

Most of the data recorded in the field test has been reduced to calibrated form and are available for general distribution. The meteorological data indicate that a fairly narrow range of air-sea temperature difference conditions, centered on -1 C, was the rule for the duration of the test. For this condition, there is a cusp-like feature in both the longwave and midwave radiance profiles at the horizon. The origin of this cusp can be understood with the aid of standard LOWTRAN modeling supplemented with model temperature profiles for the first few meters above the ocean surface. It was

possible to observe turbulence induced flicker of a point source at the horizon. High quality solar glitter field scene data were obtained.

As with any field test, the contributions of a large number of people were essential in the successful conduct of this exercise. The authors would especially like to acknowledge J. Andreotti, D. Crowder and M. Kaelberer of the Naval Systems Warfare Center, L. Brickman and C. Forsyth of Arete Associates and R. Lucke, G. Stamm and D. Spear of NRL.

6.0 REFERENCES

[1] Gathman, S. et. al. to be published

[2] Kessler, B.V. et. al., "New IRAMMP dual-band radiometric sensor", IRIA-IRIS Proceedings of 1989 Targets Backgrounds and Discrimination Meeting, Vol. I, p. 131, 1989.

[3] IRAMMP Data Catalog, Office of Naval Technology, Arlington, VA, 1990.

[4] Hughes, H.G., "Apparent infrared radiance of the sea", NOSC Tech. Rept. 1271; "Airborne FLIR detection of surface targets", NOSC Tech. Rept. 1275; "Sea and sky infrared radiances near the horizon", NOSC Tech. Rept. 1294, Naval Ocean Systems Command, San Diego, CA, 1989.

[5] Kneizys, F.X. et. al., "Atmospheric transmittance/radiance: Computer code LOWTRAN 6", AFGL-7R-83-0187, Air Force Geophysics Laboratory, Hanscom AFB, MA, 1983.

[6] Davidson, K.L., Schacher, G.E., Fairall, C.W. and Goroch, A.K., "Verification of the bulk method for calculating overwater optical turbulence", Appl. Optics vol. 20, p. 2919, 1981.

[7] Walmsley, J.L., "On theoretical wind speed and temperature profiles over the sea with applications to data from Sable Island, Nova Scotia", Atmosphere-Ocean vol. 26, p. 203, 1988.

[8] Paulus, R.A., "Specification for evaporation duct height calculations", NOSC Technical Document #1596, Naval Ocean Systems Command, San Diego, CA, 1989.

[9] Cox, C. and Monk, W., "Measurement and roughness of the sea surface from photographs of the sun's glitter", J. Opt. Soc. Amer. vol. 44, p. 838, 1954.

[10] Priest, R.G. and Schwartz, I.B., "A probabilistic model of the apparent radiance of the rough sea", NRL Memorandum Report 6092, Naval Research Laboratory, Washington, DC, 1988.

[11] Kneizys, F.X. et. al., "Users's guide to LOWTRAN 7", AFGL-TR-88-0177, Air Force Geophysics Laboratory, Hanscom AFB, MA, 1988.

[12] Hufnagel, R.E., "Propagation through atmospheric turbulence", in The Infrared Handbook, Chapter 6, ed. W.L. Wolf and G.J. Zissis, Environmental Research Institute, Ann Arbor MI, 1985.

[13] Ostrowski, P.P., Perez-Esandi, J. and Snedegar, R.W. "Naval ocean IR background analysis", Proc. SPIE, vol. 1311, p. 265, 1990.
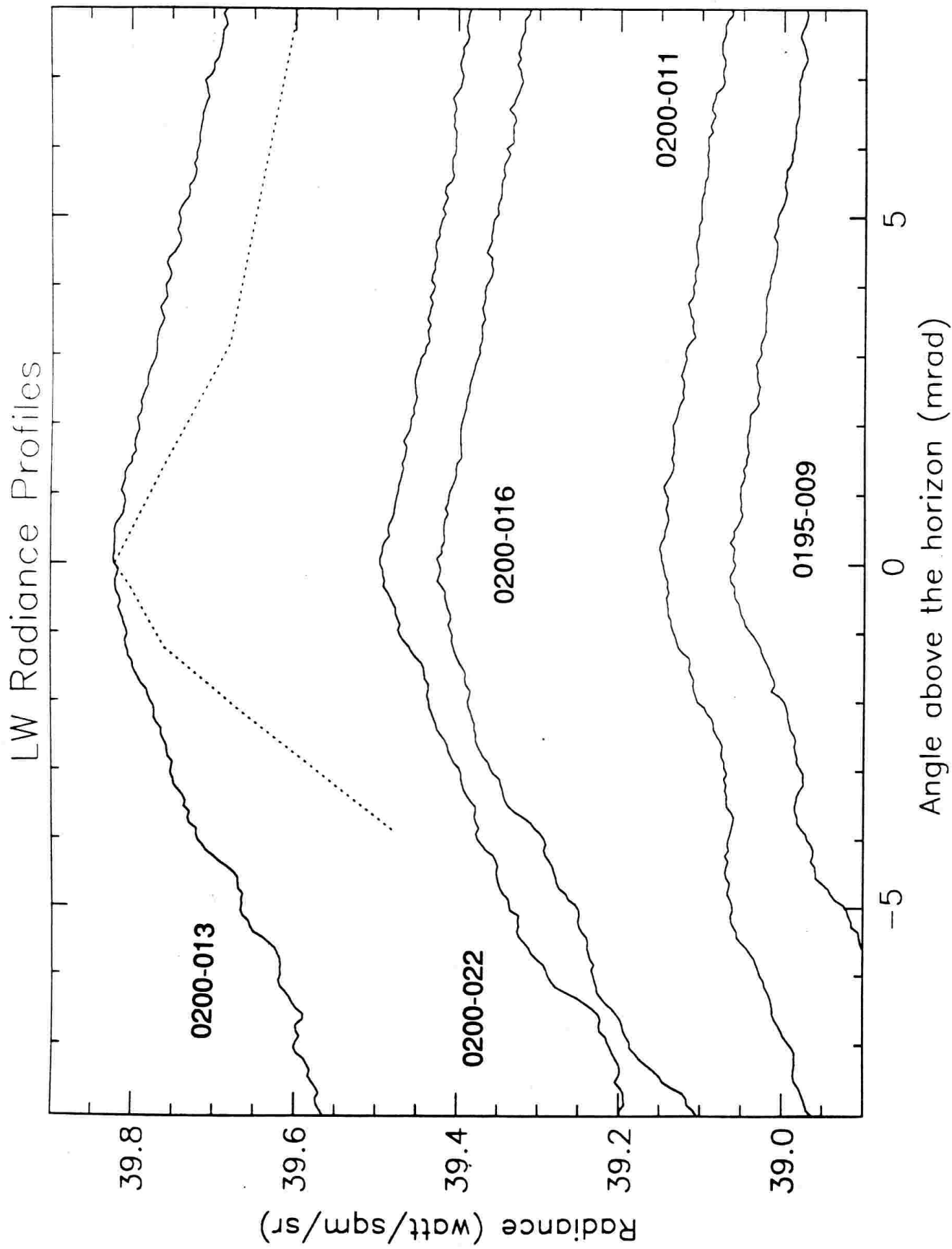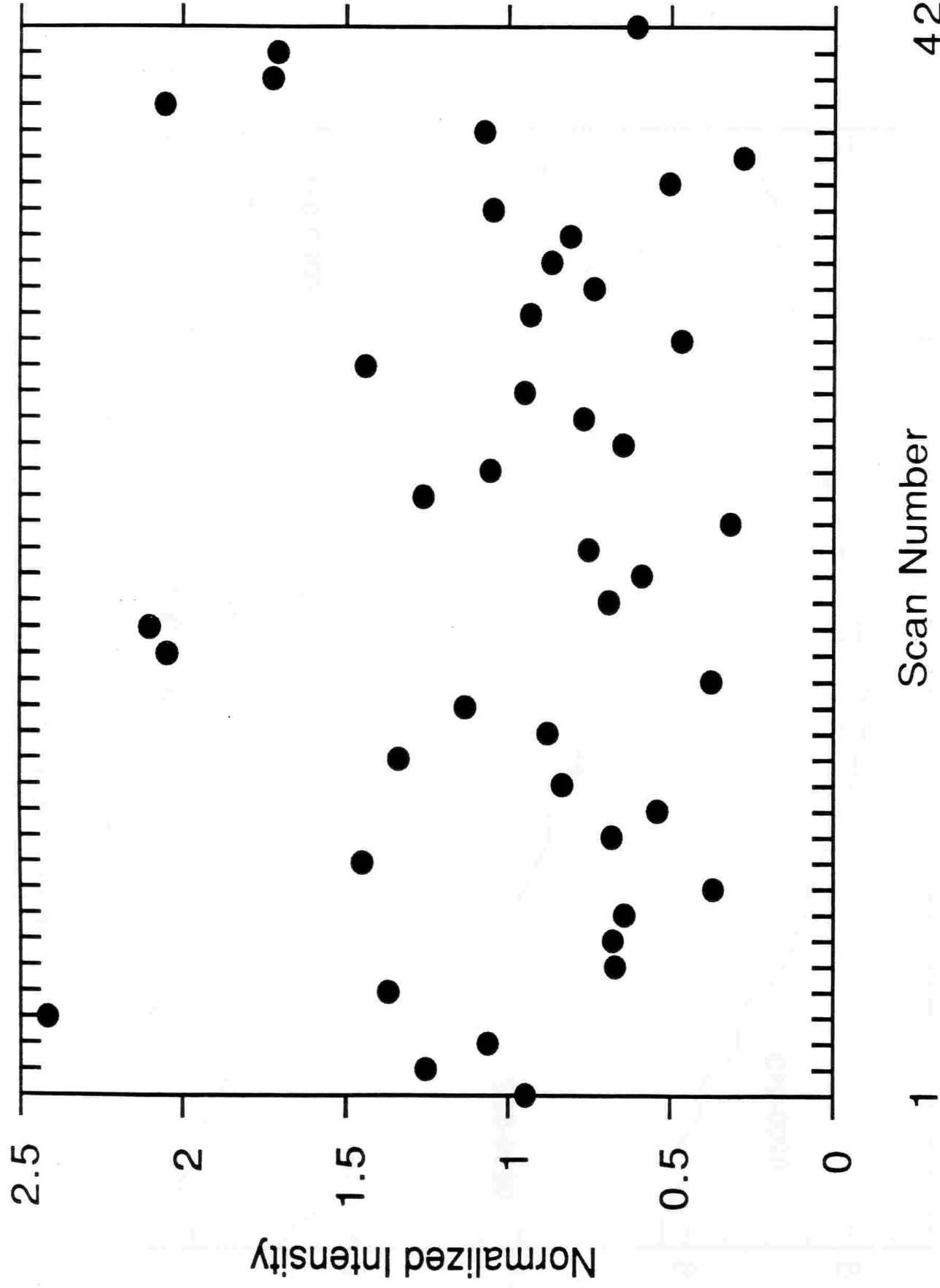
Fig. 1. Longwave radiance profiles.

Intensity Fluctuations

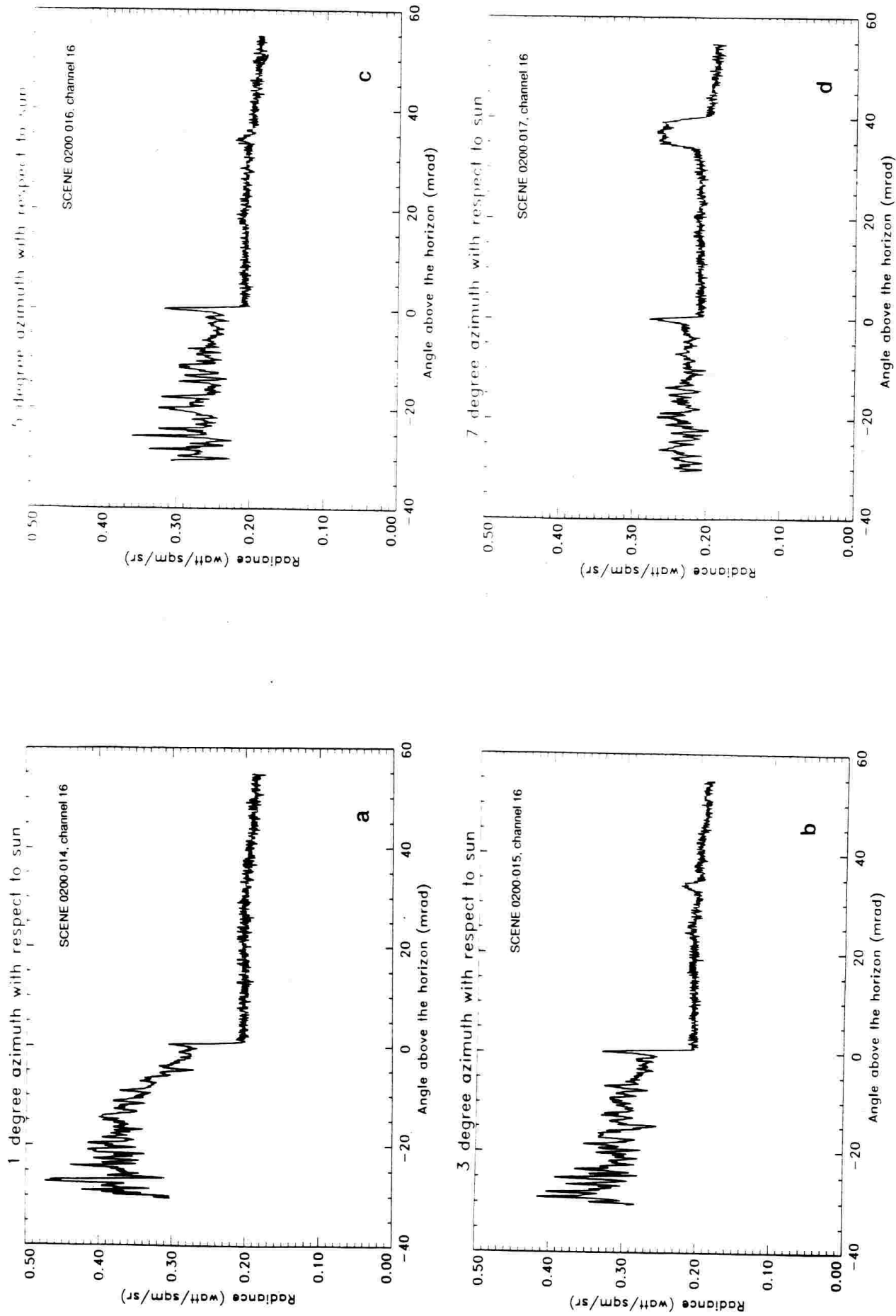Fig. 2. Normalized source intensities for scene 0198-017
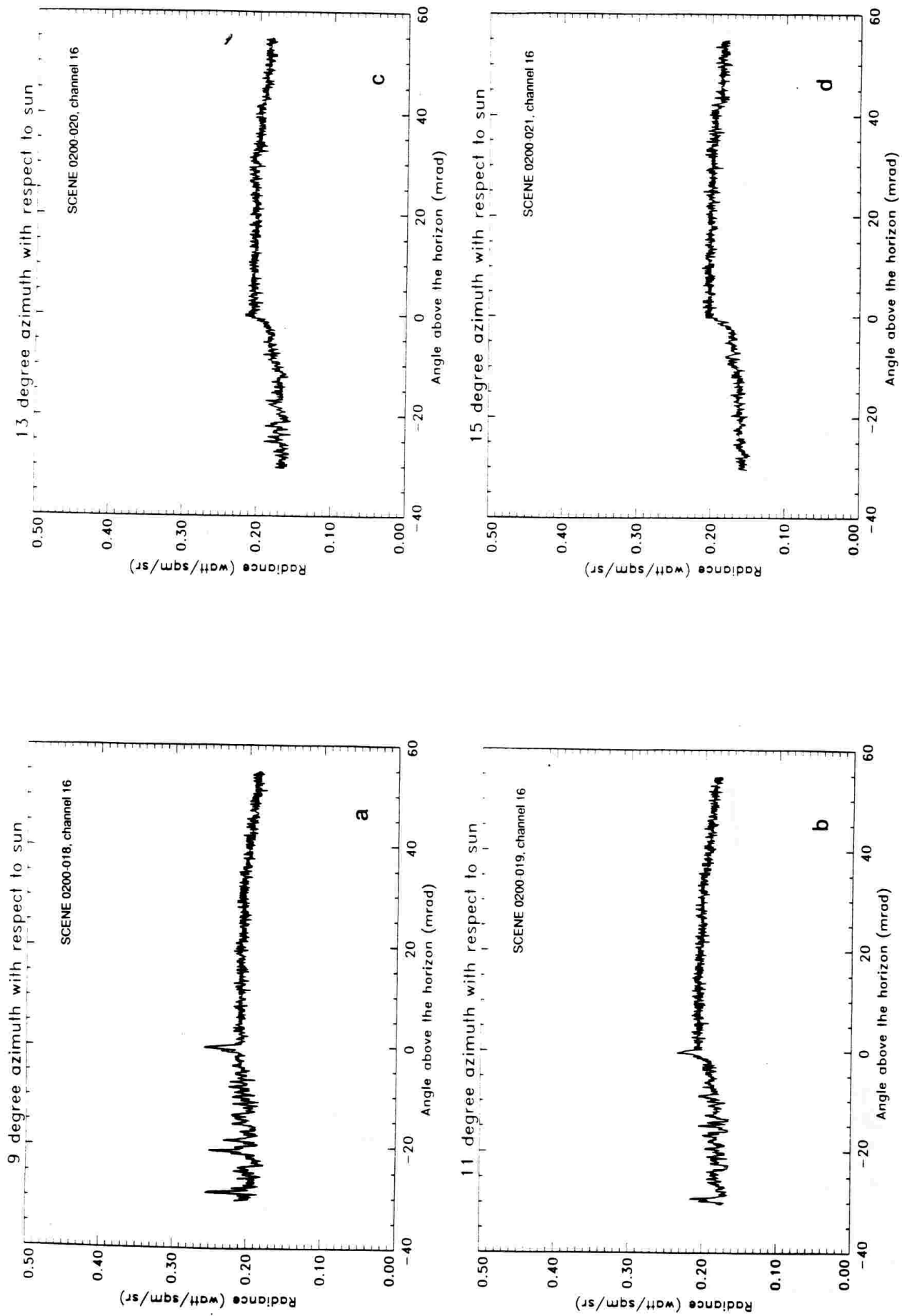
Fig. 3. Radiance profiles with solar glitter contribution

Fig. 4. Radiance profiles with solar glitter contribution